Materials Letters 120 (2014) 287–291

Contents lists available at ScienceDirect

Materials Letters

journal homepage: www.elsevier.com/locate/matlet

Mesoporous In_2O_3 with enhanced acetone gas-sensing property

Xiaohong Sun [a], Huiming Ji [a], Xiaolei Li [a], Shu Cai [a], Chunming Zheng [b,*]

[a] School of Materials Science and Engineering, Key Lab of Advanced Ceramics and Machining Technology, Tianjin University, Tianjin 300072, PR China
[b] State Key Laboratory of Hollow-fiber Membrane Materials and Membrane Processes, School of Environmental and Chemical Engineering, Tianjin Polytechnic University, Tianjin 300387, PR China

ARTICLE INFO

Article history:
Received 10 October 2013
Accepted 19 January 2014
Available online 25 January 2014

Keywords:
In_2O_3
Mesoporous structure
Sensors
Porous materials
Acetone detection

ABSTRACT

Ordered mesoporous In_2O_3 with controlled morphology have been synthesized using "container effect" nanocasting method. The mesoporous In_2O_3 with larger mesopore size and smaller particle diameter exhibited improved sensitivity (response of 29.8 to 50 ppm of acetone at 300 °C), faster response and recovery times (0.7 and 14 s) and higher selectivity to acetone. The acetone detection limit is as low as 500 ppb, which favors the precise diagnosis of human diabetes. The enhanced acetone sensing performance benefits from the large surface area with enough sensing active sites, proper pore size for sufficient gas diffusion and small particle size for effective electron depletion.

1. Introduction

Indium oxide (In_2O_3), as an important n-type and wide band-gap semiconductor (3.55–3.75 eV), is of great interest for use in electronic and optical applications, especially in resistive gas sensing, including toxic/dangerous reducing gases and oxidizing gases [1,2]. Porous structure with large surface areas and more reaction sites of In_2O_3 are supposed to enhance the gas sensing performance [3,4]. Among all kinds of preparation methods for porous In_2O_3, nanocasting synthesis of mesoporous In_2O_3 with 2–50 nm ordered pores has been proved to be an efficient way to improve the gas-sensing response, because the as-prepared In_2O_3 are with large surface-to-volume ratios and high thermal stability [5]. Tiemann's group reported the enhanced sensitivity of ordered mesoporous In_2O_3 to CH_4 with controlled pore sizes and pore wall thickness [6]. Lai et al. reported the synthesis of ordered mesoporous In_2O_3 with improved response to HCHO [7]. Pellicer's group researched the sensing properties and functional mechanism of CaO-loaded mesoporous In_2O_3 to sensing of CO_2 [8].

Acetone, as an industrial solvent and flammable gas, is also an important breath biomarker for noninvasive diagnosis of human type-1 diabetes [9]. Resistive type acetone sensors using various semiconducting metal oxides, such as WO_3 and In_2O_3, exhibit significant application on the field of biomedical, chemical industries, and personal safety, due to their real-time detection and easy miniaturization [10,11]. However, fabrication of mesoporous In_2O_3 acetone sensor with fast response time, low detection limit and high sensitivity is still a major challenge.

In this work, we synthesized ordered mesoporous In_2O_3 with different particle sizes and pore-size distributions by utilizing our previous reported "container effect" during nanocasting procedure [12]. The as-prepared mesoporous In_2O_3 were applied as a high performance gas sensor to acetone down to 500 ppb and with fast response time and high selectivity. The gas-sensing mechanism was also investigated in detail.

2. Experimental

Mesoporous In_2O_3 was synthesized using the nanocasting method with ordered mesoporous silica KIT-6 as hard template. Typically, 1.0 g $In(NO_3)_3 \cdot 5H_2O$ and 0.5 g KIT-6 were dissolved in 10.0 mL of ethanol. The ethanol was then evaporated off at 40 °C. The mixture was thermally decomposed at 400 °C for 3 h with a heating rate of 3 °C/min. KIT-6 was then removed by dissolving the In_2O_3/KIT-6 composite with hot 2 M NaOH solution twice. The remaining In_2O_3 was washed with water and dried at 60 °C. Mesoporous In_2O_3 with different particle size can be synthesized using the container effect of the thermal treatment with varied container volume [12]. In_2O_3 sample 1 was obtained by calcination in a glass bottle with volume of 350 mL, whereas sample 2 in a 30 mL glass bottle.

The wide-angle X-ray powder diffraction (XRD) pattern was recorded on a Philips X'pert powder Diffractometer with a graphite monochromator and Fe $K\alpha 1$ source ($\lambda = 0.193$ nm). The small angle X-ray diffraction (SAXRD) pattern was taken on a Philips X'pert MPD thin film powder XRD using a Cu $K\alpha$ radiation

* Corresponding author. Tel./fax: +86 22 83955661.
E-mail address: zhengchunming@tjpu.edu.cn (C. Zheng).

0167-577X/$ - see front matter Crown Copyright © 2014 Published by Elsevier B.V. All rights reserved.
http://dx.doi.org/10.1016/j.matlet.2014.01.114

(λ=0.154 nm). Transmission electron microscopy (TEM) measurements were performed on a FEI T20 microscope. The scanning electron microscopy (SEM) images were measured on a FEI XL40 instrument. Nitrogen physisorption data were measured at 77 K on a Micromeritics TriStar porosimiter apparatus. The gas sensors were fabricated by dip-coating a water paste of In_2O_3 onto alumina ceramic tube with gold electrodes. The paste was prepared by mixing of 50 mg In_2O_3 and 0.5 mL deionized water. The as-modified electrode was dried under ambient conditions overnight before use. The gas-sensing properties of the gas sensors were measured under a steady-state condition in an organic glass chamber with a volume of 20 L. An appropriate amount of gas vapor was injected into the closed chamber by a microinjector to form the prospective gas concentration. And the sensor was exposed to air again by opening the chamber when the test was completed. The gas-sensing were measured by a CGS-8 series gas-sensing measurement system (Beijing Elite Tech Co., LTD, China). The response (sensitivity, $S=R_a/R_g$) was defined as the ratio of sensor resistance in dry air (R_a) to that in a target gas (R_g).

3. Results and discussion

Fig. 1a shows the XRD pattern of In_2O_3 sample 1. Well-defined diffraction peaks indexed to the body-centered cubic (bcc) phase of bixbyite In_2O_3 (JCPDS card No. 06-0416) indicates the well crystalline nature of sample 1. The SAXRD pattern of sample 1 showing one intense peak at 2θ of 0.94° corresponds to the 211 diffraction peak of *Ia*3*d* symmetry, which indicates the long-range mesostructured regularity of hard-template KIT-6 was well

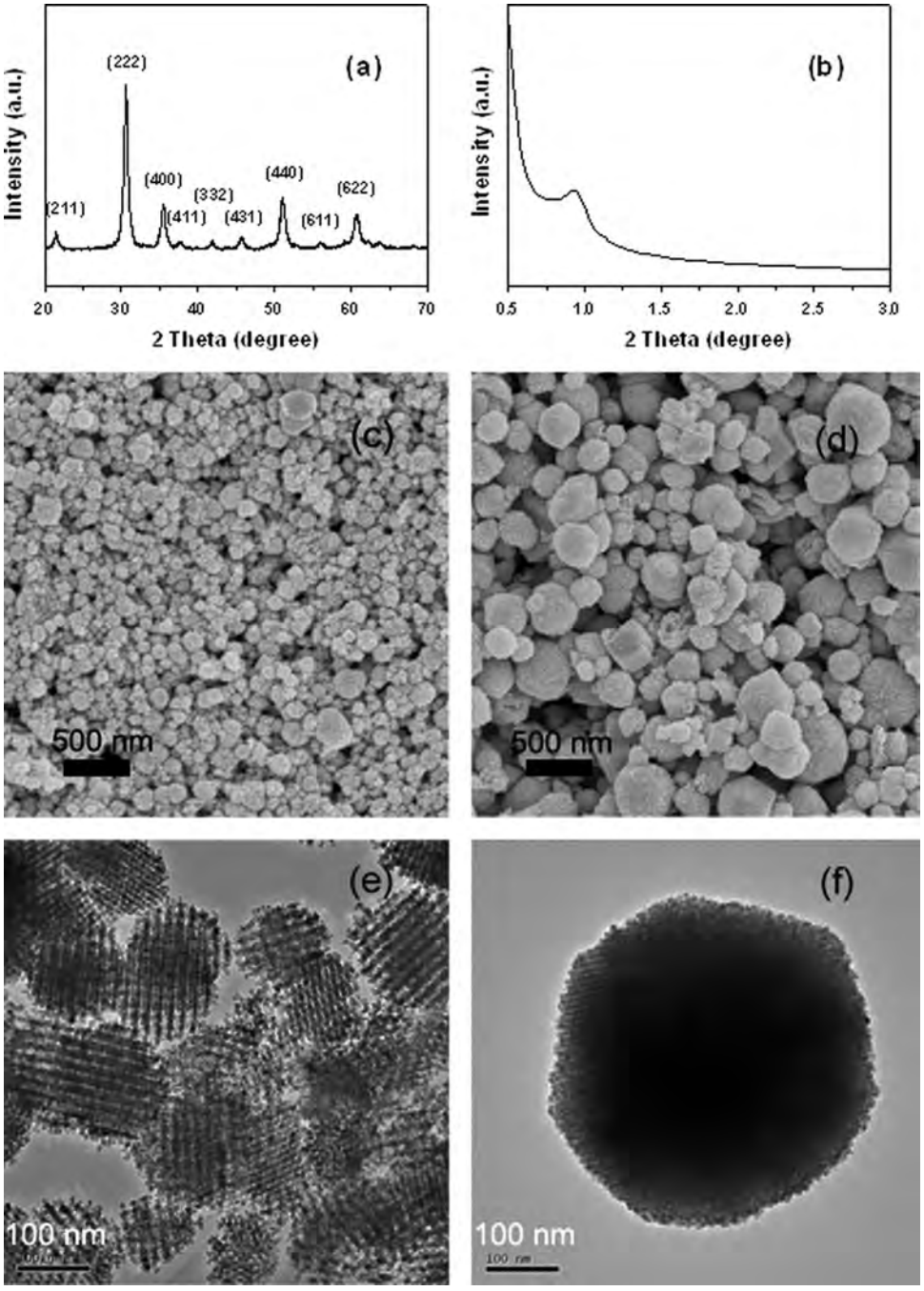

Fig. 1. XRD pattern (a), SAXRD pattern (b), SEM image (c) and TEM image (e) of In_2O_3 sample 1; SEM image (d) and TEM image (f) of In_2O_3 sample 2.

retained in the In_2O_3 replica. The SEM images of both samples are shown in Fig. 1c and d. Sample 1 is nearly spherical particle and with near uniform particle size. Sample 2 is with larger particle size and wider particle-size distribution. The average particle size of samples 1 and 2 are 135 and 346 nm, respectively, by measuring about 30 particles for each sample. Obviously, the particle sizes of the In_2O_3 can be controlled easily by our previous reported "container effect" nanocasting method [12]. The TEM images shown in Fig. 1e and f confirm that both In_2O_3 have sphere-like morphology with periodic cubic (*Ia*3*d*) mesostructure. The particle size and mesostructured ordering of sample 2 are larger than sample 1, while, sample 1 is with better particle-size distribution, which is in good agreement with the SEM result.

The optimum operating temperatures of both In_2O_3 samples were determined through varying the heating current to achieve the highest sensitivity. Fig. 2a shows the optimum operating temperature for sample 1 is 300 °C with sensitivity of 29.8 to 50 ppm of acetone, which is much higher than that (17.4) of sample 2 at the same optimum operating temperature. The response and recovery times of sample 1 to 50 ppm of acetone (Fig. 2b) are 0.7 and 14 s, respectively, which are faster than the results reported in some literatures [3,13,14], while that of sample 2 are 8 and 37 s, respectively.

Development of acetone sensor at lower detection limit and over a wide concentration range is of practical interest, especially for the diabetes diagnosis, because in exhaled breath acetone concentration increases from $\leq$900 ppb for healthy humans to 1800 ppb for diabetes patients [9]. From Fig. 2c and d it is obvious that both sensors have a wide detection range for acetone from 500 to 50 ppm. The response value to 500 ppb of acetone for sample 1 is as high as 1.8, while, that for sample 2 is 1.5. With the increasing of the acetone concentration, the responses greatly increase. Fig. 2e show that sample 1 is more sensitive than sample 2. When compared with other reported In_2O_3 acetone sensors [13,14], sample 1 still possesses superior performance with a sensitivity of 29.8 to 50 ppm of acetone. Fig. 2f illustrates the response of both In_2O_3 to 50 ppm of various gases. Obviously, the responses of sample 1 to five gases are all better than that of

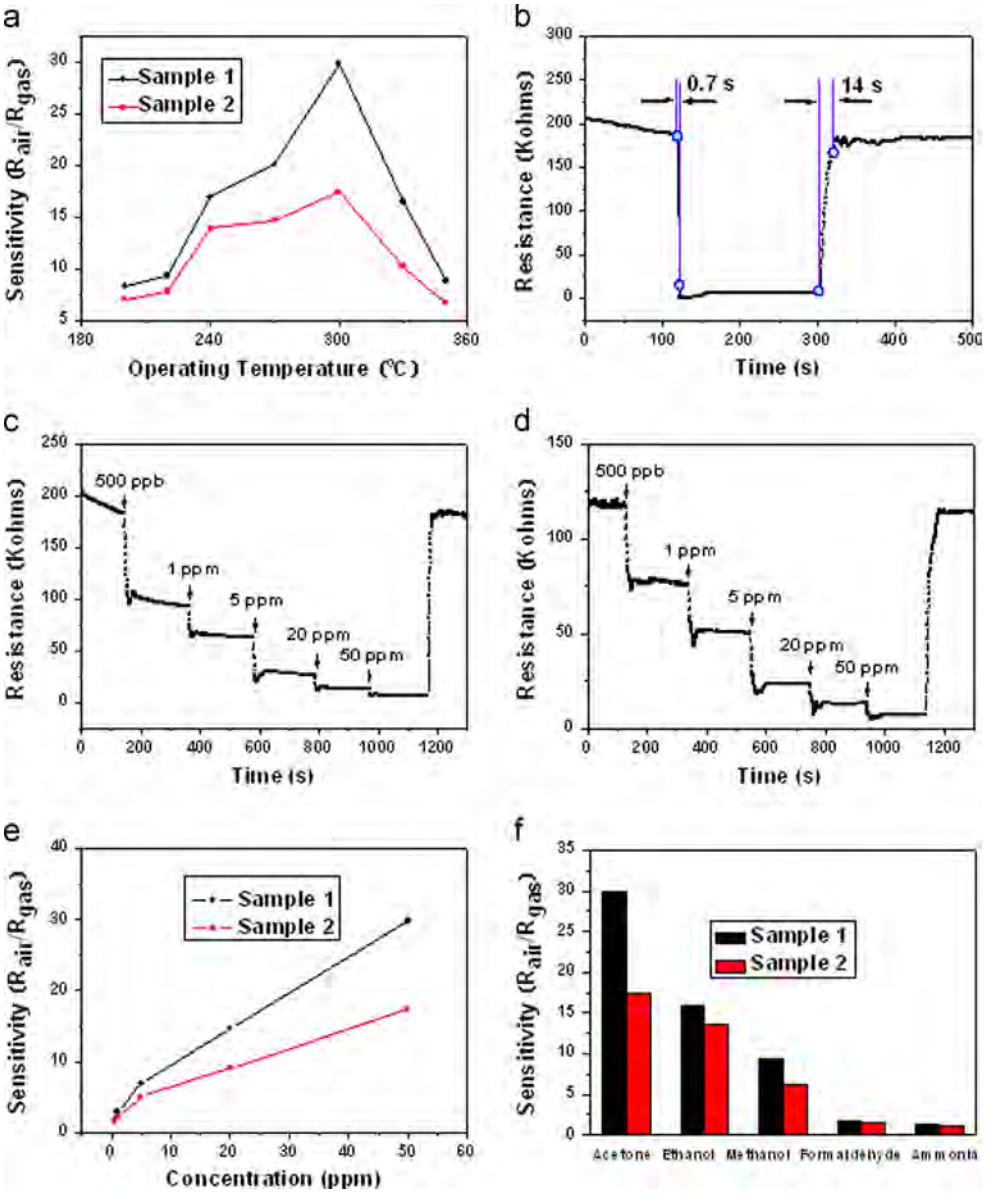

Fig. 2. The sensitivity versus operating temperature of both In_2O_3 to 50 ppm of acetone (a); dynamic sensing transient of sample 1 to 50 ppm of acetone at 300 °C (b); typical response and recovery curves to different acetone concentration of sample 1 (c) and 2 (d); sensitivity of both In_2O_3 with varied acetone concentration (e); sensitivity values of both In_2O_3 to 50 ppm of various gases (f).

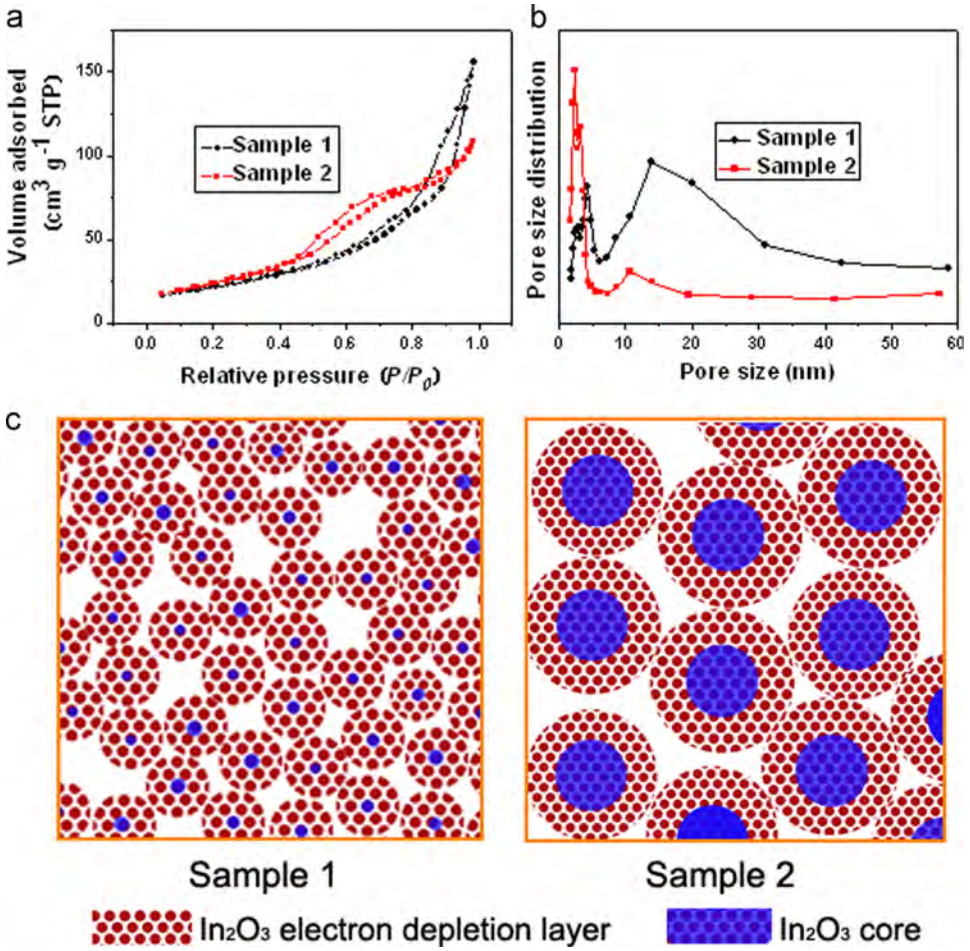

Fig. 3. Nitrogen physisorption isotherms (a) and pore size distributions (b) of both In_2O_3; sensing mechanism of both In_2O_3.

sample 2, and the largest increase is observed for acetone, implying the good selective detection of the sample 1 sensor to acetone.

When working at the optimal operation temperature of 300 °C, sample 1 has the better sensitivity to acetone in compared with sample 2. For metal oxide sensor, the sensing performance depends on several factors, such as surface areas, porous structures and particle sizes, which greatly affect the adsorption and diffusion of gas molecules [15]. The N_2 physisorption results are shown in Fig. 3a and b. Both samples gave a typical IV isotherm with a clear H1-type hysteresis loop, which is characteristic for mesoporous materials. The specific surface areas of sample1 and 2 are 77.2 and 87.5 $m^2\ g^{-1}$, respectively. The average pore sizes of sample 1 are 4.4 and 13.9 nm, which arise from the KIT-6 replica and the piled porosity by the particles aggregation, respectively, whereas for sample 2, the average pore size of 2.3 and 10.6 nm can be observed. Sample 1 and 2 are with the similar mesoporous morphology except for their particle size and pore-size distributions. Tiemann et al. indicated that Knudsen diffusion is the main diffusion type for metal oxide sensing materials with smaller pores sizes (several nanometers), and the bigger pores are favorable for the transport of gas molecules [4]. Sample 2 with larger particle size decreases the proportion of larger piled mesopores (Fig. 3b), makes the diffusion of target gases within the sensing layer hard, and results the short effective diffusion and thin electron depletion layer, which leads to the lower gas sensitivity performance (gas-sensing mechanism in Fig. 3c). For sample1, proper diffusion channel of small intraparticle mesopores and big interparticle mesopores, and moderate particle size for effective electron depletion are all causes for the best sensor response, even with a little lower surface area compared to sample 2.

4. Conclusions

In this study, ordered mesoporous In_2O_3 with different particle size and pore-size distribution have been synthesized using "container effect" nanocasting method. The In_2O_3 gas sensors were evaluated by changing the operation temperature, gas concentration and gas species. In_2O_3 sample 1 with 135 nm in particle size and 4.4 and 13.9 nm in pore sizes exhibited high sensitivity, low detection limit and good selectivity to acetone. A possible enhancement gas-sensing mechanism was also proposed based on the In_2O_3 morphology and gas-sensing properties.

Acknowledgements

This work was supported by the NSFC (51172157, 51202159, 51208357, 51372166), Doctoral Program of Higher Education, Ministry of Education (20120032120017), General Program of Municipal Natural Science Foundation of Tianjin (13JCYBJC16900, 13JCQNJC08200).

References

[1] Lee JH. Sens Actuators, B 2009;140:319–36.
[2] Xu L, Song HW, Dong B, Wang Y, Chen JS, Bai X. Inorg Chem 2010;49:10590–7.

[3] Zhang T, Gu FB, Han DM, Wang ZH, Guo GS. Sens Actuators, B 2013;177:1180–8.
[4] Tiemann M. Chem Eur J 2007;13:8376–88.
[5] Korotcenkov G, Cho BK. Crit Rev Solid State Mater Sci 2010;35:1–37.
[6] Waitz T, Wagner T, Sauerwald T, Kohl CD, Tiemann M. Adv Funct Mater 2009;19:653–61.
[7] Lai XY, Wang D, Han N, Du J, Li J, Xing CJ, et al. Chem Mater 2010;22:3033–42.
[8] Prim A, Pellicer E, Rossinyol E, Peiro F, Cornet A, Morante JR. Adv Funct Mater 2007;17:2957–63.
[9] Righettoni M, Tricoli A, Pratsinis SE. Anal Chem 2010;82:3581–7.
[10] Wang L, Teleki A, Pratsinis SE, Gouma PI. Chem Mater 2008;20 (4794 – 1496).
[11] Choi SJ, Lee I, Jang BH, Youn DY, Ryu WH, Park CO, et al. Anal Chem 2013;85:1792–6.
[12] Sun XH, Shi YF, Zhang P, Zheng CM, Zheng XY, Zhang F, et al. J Am Chem Soc 2011;133:14542–5.
[13] Zai JT, Zhu J, Qi RR, Qian XF. J Mater Chem A 2013;1:735–45.
[14] Dong HX, Liu Y, Li GH, Wang XW, Xu D, Chen ZH, et al. Sens Actuators, B 2013;178:302–9.
[15] Wagner T, Haffer S, Weinberger C, Klaus D, Tiemann M. Chem Soc Rev 2013;42:4036–53.